ANALYSIS ON THE MECHANICS AND DEFORMATION OF SIDE PILE STRUCTURE IN METRO STATION WITH THE PBA METHOD

Jianguo Gao1, Zhaofa Zeng1, Shuai Zhang2, Huijian Zhang2 and Xuemin Zhou2

1.   *Guangzhou Metro Construction Management Co. Ltd, Guangzhou, 510330, China*

2.   *School of Civil Engineering, Key Laboratory of Transportation Tunnel Engineering, Ministry of Education, Southwest Jiaotong University, No. 111, North Section, Second Ring Road, Jinniu District, Chengdu, Sichuan Province, 610031, China; 1165981488@qq.com; huijianz@163.com; xm.zhou@my.swjtu.edu.cn*

ABSTRACT

There is limited research on the interaction mechanism between the buckling load of the side pile top and the soil pressure behind pile (SPP) with the side pile. As the side pile serves as a crucial component of the lining structure in the metro, using the pile-beam-arch (PBA) method, it plays a vital role in maintaining the mechanical stability and deformation control of the station's lining system. Based on the Guangzhou Metro Line 11 project, this paper delves into the impact of mechanical characteristics and deformation of the side pile using the PBA method. It considers various factors such as different buckling loads, including horizontal load of arch (HLA), vertical load of arch (VLA) and SPP and offers corresponding construction suggestions. Our findings indicate that the lateral displacement and deformation of the side pile are primarily influenced by the HLA. The optimal HLA value stands at 1200kN. As the HLA increases, the side pile undergoes a transformation from a forward-inclined deformation mode to a belly distension deformation mode when moving towards the station's interior. The influence of HLA on bending moments about the side pile surpasses that of axial force. The VLA exerts a more significant effect on vertical settlement of the side pile, yet its impact on lateral pile body deformation is minimal. An increase in HLA significantly impacts the axial force of the side pile, but has minimal effects on bending moments. The SPP holds significant influence on the stability of the side pile; hence, it is recommended to implement appropriate lining measures to guarantee stability when dealing with exceptionally high SPP values.

KEYWORD

PBA method, Side pile, Mechanical properties, Deformation law

INTRODUCTION

The stability of underground structures has always been a key area of research [1-4]. The PBA method, which was refined by Chinese engineers based on the shallow-buried excavation method by combining the technical achievements of cover excavation and frame structures, has

been successfully implemented in the construction of subway stations across numerous cities in China [5-7]. The core of PBA method is to form a lining structure system of underground with pile-beam-arch interaction through the organic combination of small pilot tunnel, arch, lining pile and other mature technologies, which can withstand the external load during the construction of underground station and form a strong and effective safe working space under its protection. This construction method has unique advantages such as remarkable control effect of surface settlement, flexible structure, high construction safety, and small influence on the nearby environment [8, 9]. So it is especially suitable for urban subway station construction projects with large surface traffic flow, complex and variable underground pipelines, limited construction sites, and high requirements of ground settlement [10-12].

During the construction of stations using the PBA method, the side pile emerges as a crucial element of the station's lining system [13]. Its functionality extends beyond merely transferring the upper load to deeper soil layers; it also serves to restrict lateral deformation triggered by station excavation. Presently, investigations into pile stress mechanisms are predominantly focused on projects involving foundation reinforcement [14-17], foundation pit lining [18-20], slope stabilization [21-24], and other related fields. Based on the foundation pit project of an underground passage, He [25] analyzed the impact about various CFG composite foundation parameters on the deformation of the envelope structure. It was found that CFG pile composite foundation can not only reduce the vertical displacement of soil, but also reduce the lateral deformation of soil. An *et al.* [26] studied the bearing characteristics of high-pressure rotating pile when strengthening soft soil foundation, analyzed the mechanism of pile group in reducing soil settlement and improving the bearing capacity of foundation. It was pointed out that high-pressure rotating pile can significantly control soil deformation from the depth of the surface to the bottom of the pile, and increase the pile diameters and material strength about pile can significantly increase the carrying capacities about composite foundation. Wang [27] studied the differences in the strengthening effects of high-pressure rotating pile, pit static pile and manual excavation pile on loess foundation, and found that manual excavation pile has the characteristics of high bearing capacity in single pile, good reinforcement effect, reliable construction quality, and obvious advantages in the reinforcement of collapsible loess. Liu *et al.* [28] investigated the effects of pile and cushion parameters on the deformation about composite foundation using deep mixed pile, and found that pile length has the most significant effect on controlling the deformation about composite foundation, while elastic modulus of cushion has little effect on it. Benmebarek *et al.* [29] demonstrated that free piles make little contribution to increasing the safety factor about the viscous-friction slope, and the pile arching effect would completely disappear due to soil flowing effect between piles when the pile spacing ratio is greater than four. Chen *et al.* [30] put forward a correction method for the ultimate lateral soil resistance of rigid piles in non-cohesive soil of slope, pointing out that in shallow soil layer, the lateral soil resistance gradually increased with the depths, and the lateral resistance of soil reduced with the increase of slope angle and reached the limit value more easily. To sum up, some scholars have conducted certain studies on the bearing capacity and mechanical performance of lining piles. And many important results have been obtained, mostly in the aspects of composite foundation, foundation pit, slope and so on. The unique mechanical nature of the side pile in the metro system utilizing the PBA

method differs significantly from the conventional vertically stressed pile and the lining pile that solely experiences lateral load. Therefore, it cannot be accurately analyzed using current calculation methods, and existing research results cannot be simply applied when dealing with the problem of the side pile in metro with PBA method.

Therefore, relying on the Tianhe East Station project of Guangzhou Metro Line 11 (constructed by PBA method), this paper studies the mechanical characteristics and deformation rules of the side piles of station under different key construction stages by using numerical calculation method, considering the influence factors such as different HLA, VLA and SPP, aiming to provide some important guidance for similar project.

PROJECT OVERVIEW

Guangzhou Metro Line 11 is a downtown metro line, and its total length is 43.2 kilometers. Tianhe East Station is the 7th station of Guangzhou Metro Line 11. It is laid under the surface of Tianhe North Road, as displayed in Figure 1 (a). The station belongs to a two-span station with one column and two underground layers, which is constructed by PBA method. The height, width and depth of the station is 21.4m, 25.5m and 9m, respectively. The side piles are in the form of manual excavation pile with the size (pile diameter × pile distance × pile length=1.2m × 1.5m × 15m). The cross-sectional arrangement of the station structure is displayed in Figure 1 (b). According to the site survey data of Guangzhou Metro Line 11, the side piles of the station are mainly located in the following three typical strata: strong weathering argillaceous siltstone, medium weathering argillaceous siltstone and breezy gravel coarse sandstone.

(a) Geographical location of the Guangzhou Metro Line 11
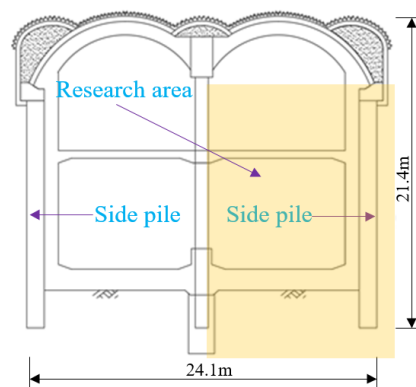
(b) Cross-sectional picture of the Tianhe East Metro Station

Fig. 1 - Basic overview of the Tianhe East Metro Station

CALCULATION INSTRUCTIONS

Calculation model

FLAC3D finite difference software is adopted for numerical simulation, and the relevant physical and geometric parameters about the calculation models are used through the actual

engineering data of Guangzhou Metro Line 11, and the established finite element model is displayed in Figure 2. For the boundary size about the model, in order to decrease the impact about "boundary effect" on the calculation results, the model size is width × height × longitudinal length = 72m×35m×21m. The normal displacement constraint is applied to the bottom and horizontal surrounding boundary of the model, and the load boundary is applied to the top to simulate the actual buried depth of the metro station. This paper uses the attach command method and the setting of common node recommended in the FLAC3D software [31] to define the contact of different components.
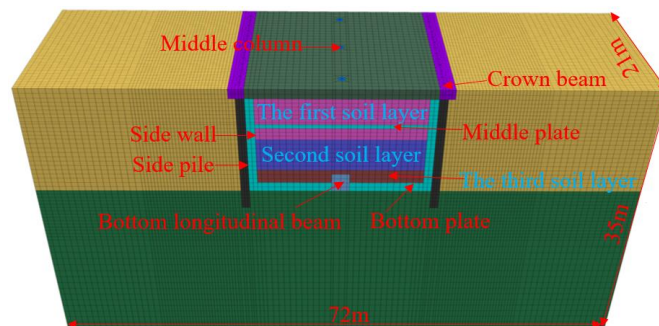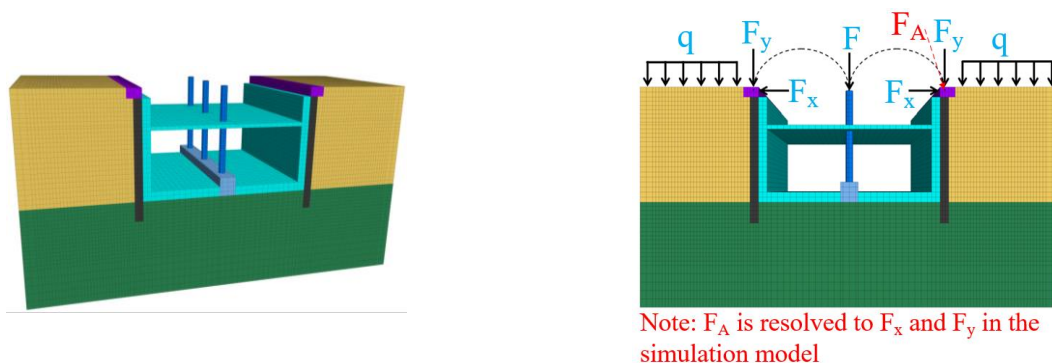

Fig. 2 - Numerical calculation model

Based on the principle of mechanical equivalence, the calculation model is simplified. The buckling force F_A of the arch of station is decomposed into VLA (F_y) and HLA (F_x) applied to the crown beam and mid-column structure, and a uniform load SSP (q) is imposed on the soil surface behind the pile to simulate the overlying soil pressure. The simplified calculation models are displayed in Figure 3. According to the calculation results from the bedded-beam model, it is obtained that the VLA and HLA of the crown beam structure are 1200kN/m and 800kN/m respectively. The VLA of the two arches on both sides of the mid-column structure is borne within 8m column spacing, and the HLA will cancel each other due to the symmetry of the left and right arches. It is calculated that the load (F) of the top of single column is 19200kN, and the SSP is 250kPa.

Note: F_A is resolved to F_x and F_y in the simulation model

(a) Detail model of the station   *(b) Simplification diagram of the load of arch*

Fig. 3 - The simplified calculation models

Numerical simulation of the simplified PBA method

In this paper, the numerical simulation process of PBA method is carried out according to steps (a) ~ (i) : (a) Initial geostress equilibrium; (b) Application of the q; (c) Installation of side piles, crown beams, and middle columns; (d) Application of F_x and F_y to the crown beam and F to the middle column; (e) Excavation of the first soil layer of the main body of the station; (f) Installation of the center plate and side wall corresponding to the position of the first soil layer; (g) Excavation of the second soil layer of the main body of the station; (h) Excavation of the third soil layer of the main body of the station; (i) Installation of the bottom plate, bottom stringer and side wall. The main structure of the station has been completed.

Computation parameter

The surrounding rock as well as the lining structure of the station are simulated by solid elements, and the surrounding rock adopts the ideal elastic-plastic constitutive model and obeys the Mohr-Coulomb strength yield criterion [32, 33]. The lining structure is regarded as linear elastic material and adopts elastic constitutive model. The calculation parameters about surrounding rock as well as lining structure of the station are displayed in Table 1 and Table 2.

Tab. 1 - Calculation parameters about surrounding rock

Name	Density ρ /(kg/m^3)	Elastic modulus E /MPa	Cohesive force c /kPa	Friction angle φ /°	Poisson's ratio μ
Highly weathered argillaceous siltstone	2100	120	50	28	0.33
Medium weathered argillaceous siltstone	2500	500	150	30	0.25
Breezy gravelly coarse sandstone	2600	2000	260	32	0.25

Tab. 2 - Calculation parameters about station lining structure

Name	Lining material	Size	Density ρ /(kg/m^3)	Elastic modulus E /GPa	Poisson's ratio μ
Crown beam	C30 reinforced concrete	1.8×1.2m	2500	30.0	0.20
Middle column	C50 reinforced concrete	0.9m@8m	2700	63.5	0.20
Bottom longitudinal beam	C35 reinforced concrete	1.4×2.9m	2700	31.5	0.20
Sidewall	C35 reinforced concrete	Thickness =0.8m	2700	31.5	0.20

Middle plate	C35 reinforced concrete	Thickness =0.5m	2700	31.5	0.20
Bottom plate	C35 reinforced concrete	Thickness =1.2m	2700	31.5	0.20

Calculation conditions

The side pile is the key stress component in the lining structure with PBA method, which plays a vital role in the mechanical stability and displacement control about the lining system of station. Its stress state is not only related to the properties of the strata around the pile, but also closely related to the mechanical state about pile top (HLA and VLA), and the SPP (manifested by buried depth) and other factors. The load mode of the side pile is different from the bearing pile which mainly bears vertical load and the supporting pile which mainly bears lateral load. The pile top bears the load transmitted by the arch, and the pile body bears the lateral soil pressure caused by the soil behind the pile. However, at present, the theoretical research of station with PBA method still lags behind the practical experience of engineering, especially the interaction mechanism between the pile top buckling load (HLA and VLA) and the SPP and side pile is rarely involved, and the law of its influence on the mechanics as well as deformation about side pile is not completely clear. Based on this, this paper studies the mechanical characteristics as well as deformation laws about pile structure under different loads through changing these three main influencing factors (HLA, VLA and SPP). The specific calculation conditions are displayed in Table 3.

Tab. 3 - Calculation conditions

Influencing factor	Conditions				Instructions
HLA /(kN/m)	400	800	1200	1600	Fix VLA =1200 kN/m and SPP =250 kPa
VLA /(kN/m)	800	1200	1600	2000	Fix HLA =800 kN/m and SPP =250 kPa
SPP /kPa	125	250	375	500	Fix VLA=1200 kN/m and HLA =800 kN/m

ANALYSIS OF THE CALCULATION RESULTS

Influence of HLA on side pile

Deformation analysis of side piles

The evolution rule about lateral displacements of lower pile structure under different HLAs with the station construction process is displayed in Fig. 4. ***Note:*** for the description of convenience, the main construction stages are represented by stages A~D, namely, stage A (completion of the buckle arch), stage B (excavation of the 1st layer), stage C (excavation of the 2nd layer), stage D (completion of the bottom plate).
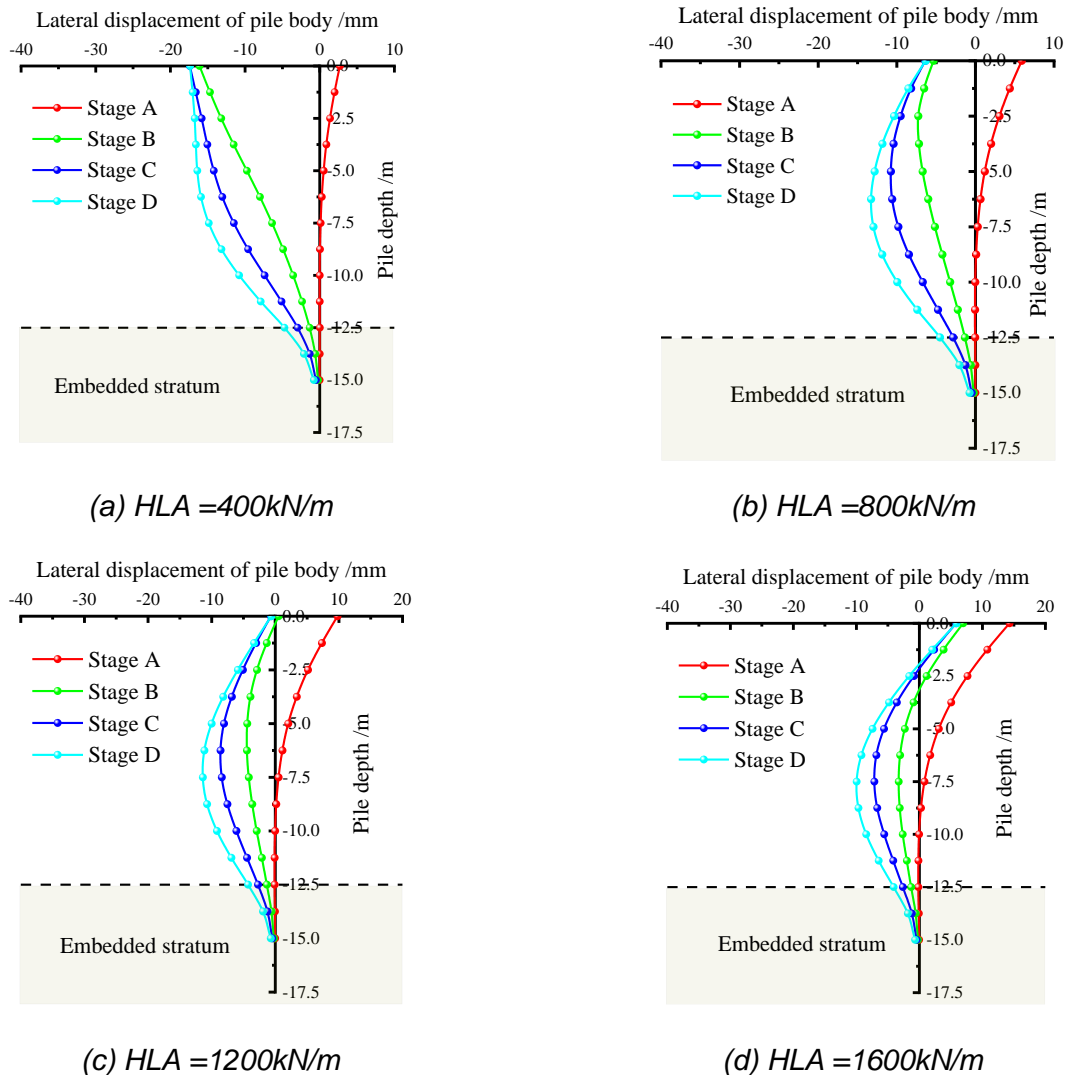
(a) HLA =400kN/m

(b) HLA =800kN/m

(c) HLA =1200kN/m

(d) HLA =1600kN/m

Fig. 4 - Evolution law of the lateral displacement about pile under various HLA

In Figure 4, since the side pile is similar to the cantilever beam structure after the completion of the buckle arch, under the action of HLA, the pile body generates a positive displacement to the outside of the station, and the value of the positive displacement increases with the HLA. Under each condition (HLA =400~1600 kN/m), the maximum lateral displacements about the pile body after the completion of the buckle arch appears at the top of the pile, and its displacement value is 2.71mm, 5.91mm, 9.80mm and 14.32mm in order. In other words, the greater the HLA, the greater the lateral displacements about the pile, and the more adverse it is to the side pile. Subsequently, with the excavation of soil inside the station, the side pile gradually migrates to the station, but the lateral deformation trend and amplitude of the pile body are different due to the different HLA on the pile top. For the HLA is small (only 400kN/m), when excavating the 1st soil layer, due to the excavation about the soil inside the station, the soil stresses on the pile side are released, and the lateral displacement about the pile body quickly changes from the "forward" deformation mode after the completion of the arch to "backward" deformation mode. The largest lateral displacements about the pile body still appears at the pile top, and the displacement changes greatly (up to 18.80mm). Once

the HLA increases to be more than 800kN/m, due to the large HLA on the pile top, the pile plays a better lateral lining role, resulting in the deformation characteristics about the side pile from "forward" mode to "bulging" mode when it migrates to the station interior. The results reveal that the lateral displacements about side piles are significantly affected by the HLA. When the HLA is small, the pile top cannot form good horizontal lining effect, and is prone to large deformation, which is not conducive to the stability of side pile.

The final lateral displacements of side pile under different HLA after the completion of station construction are shown in Figure 5, and the final peak lateral displacements of side piles are extracted, as shown in Table 4.
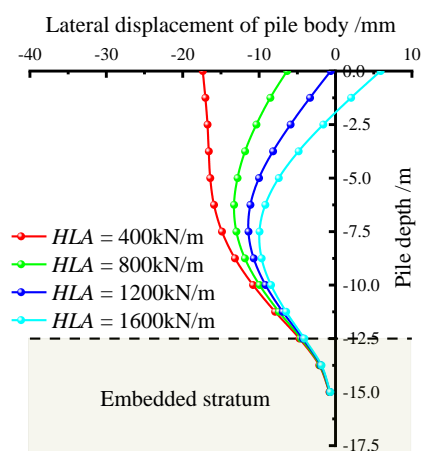
Fig. 5 - Comparison of the final lateral displacement of pile body

Tab. 4 - Peak value of the final displacement of pile body under different HLA /mm

Lateral displacement X	HLA = 400kN/m	HLA = 800kN/m	HLA = 1200kN/m	HLA = 1600kN/m
Maximum value X_{max}	-0.78	-0.74	-0.61	5.92
Minimum value X_{min}	-17.37	-13.27	-11.38	-9.94
Relative difference X_d	16.59	12.53	10.77	15.86

Note: the relative difference ($X_d = X_{max}-X_{min}$) about lateral displacements of pile body is adopted to describe the bending degree of pile body.

In Figure 5 and Table 4, with the adding of HLA, the constraint effect on side pile is enhanced, the lateral displacements about pile body gradually decreases, and the deformation characteristics also change, indicating that HLA imposes a crucial role in the lateral displacement about side pile. When the HLA ranges from 400kN/m to 1600kN/m, the peak lateral displacement of side piles are -17.37mm, -13.27mm, -11.38mm and -9.94mm, respectively. The difference between the two adjacent lateral displacement peaks is 4.10mm, 1.89mm and 1.44mm, which indicates that the lateral displacement about the pile gradually decreases with the increasement of the HLA, while the displacement reduction rate gradually decreases, and the controlling effect on the lateral

displacement is gradually weakened. With the increasement about HLA, the relative differences about pile lateral displacements decrease first and then increases. The greater the relative differences about lateral displacements of side pile, the more serious the bending degree of side pile. The minimum relative difference about lateral displacements of pile body occurs when the HLA is 1200kN/m, and the relative difference is only 10.77mm, which indicates that the HLA has a relatively optimal value on the bending deformation about pile. Whether the HLAs are too large or too small, the side piles are prone to produce large bending deformation of pile body, resulting in structural damage, so the influence of HLA on structure should be considered in the design of side pile.

The variation law about the deformation of pile top with HLA after the completion of station construction is shown in Figure 6.
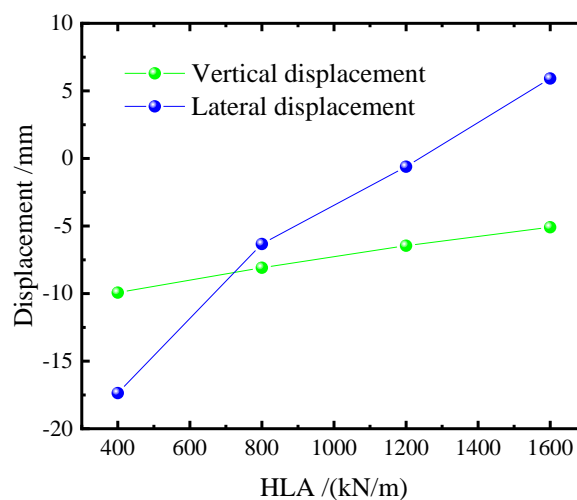
Fig. 6 - Variation law of the deformation about pile top with various HLA

In Figure 6, under constant VLA, the vertical settlement of pile top reduces with the increase of HLA. The reason is the lateral lining effect of HLA on pile top, which increases the contacting stresses between side pile and soil around the pile, resulting in a gradual increase in the side friction resistance about pile borne by side pile, thus reducing the vertical settlement of side pile. When the HLA increases to 1200kN/m, the lateral displacements about pile top changes from negative displacements inside the station to positive displacement outside the station, which indicates that HLAs play a vital role in deformation about pile top and should be paid more attention to it. It is worth mentioning that the vertical displacement and horizontal displacement are equal around HLA=700kN/m. This is because the main control factor in this section is HLA (i.e., horizontal force). With the increase of HLA, the horizontal displacement of pile top significantly decreases, while the vertical displacement of pile top is less affected by this.

Analysis of the variation law about internal force of pile

The variation law of internal forces of the lower pile structure under different HLA during the construction process is displayed in Figures 7~8. The final distribution about the comparison diagram of internal forces and peak value of side pile after the completion of station construction are shown in Figure 9.
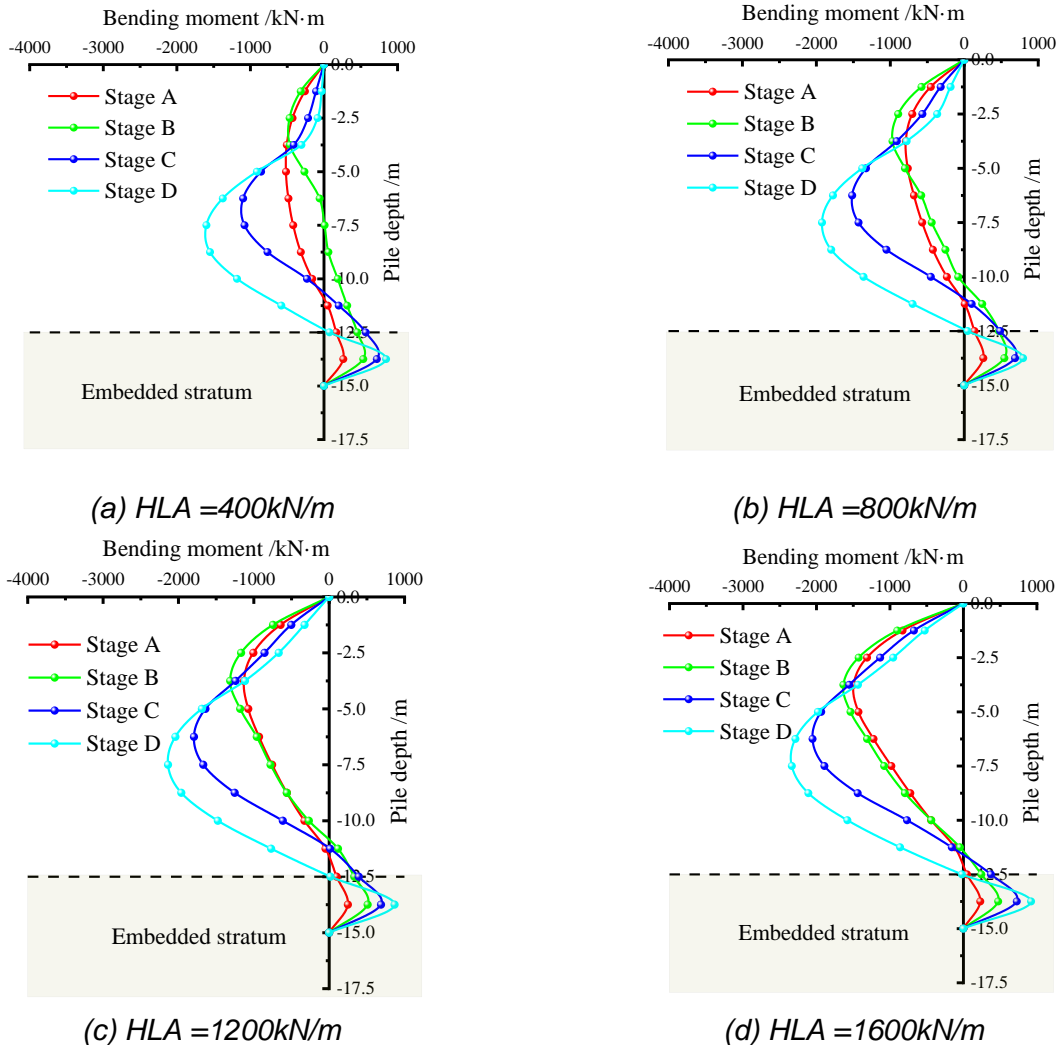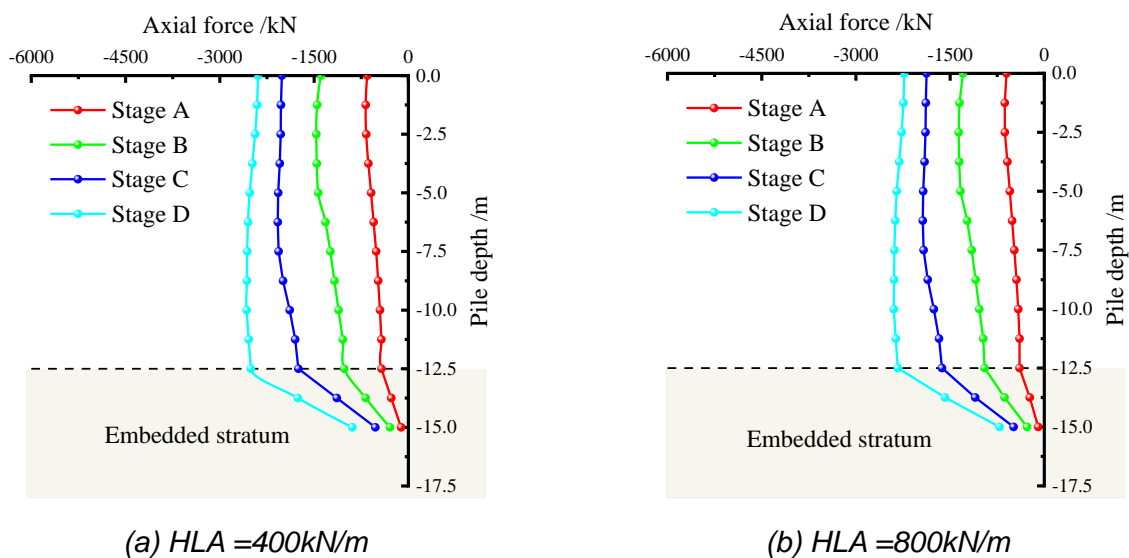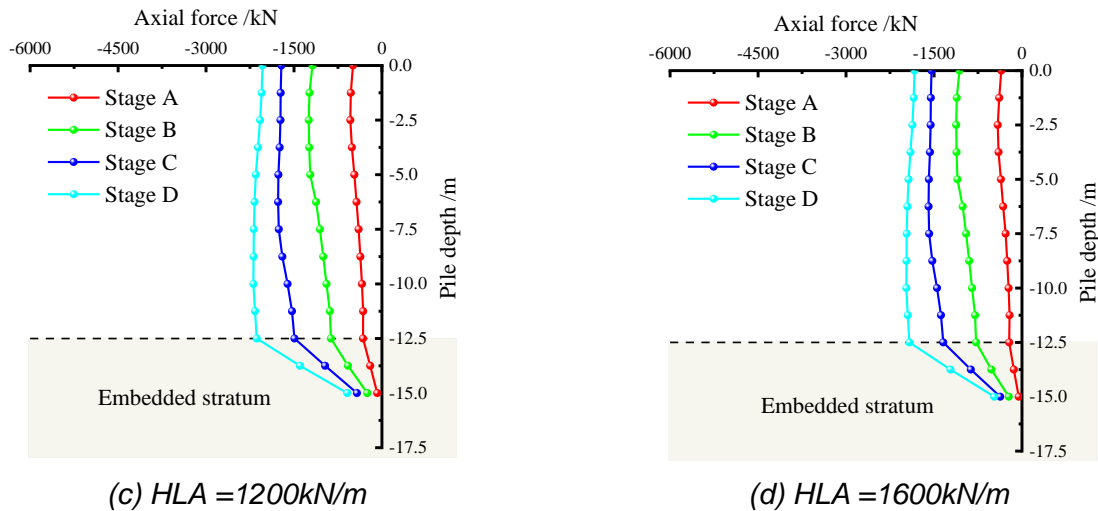
(a) HLA =400kN/m

(b) HLA =800kN/m

(c) HLA =1200kN/m

(d) HLA =1600kN/m

Fig. 7 - Evolution of the bending moments about side pile under different HLA

(a) HLA =400kN/m


(b) HLA =800kN/m

(c) HLA =1200kN/m   *(d) HLA =1600kN/m*

Fig.   8 - Variation law of the axial forces about side piles under various HLA

In Figures. 7~8, during the construction of the station, the bending moments about the pile are basically presented as "bow" distribution with large in the middle and small at both ends. The pile part above the excavation faces about the soil is mainly strained on the excavation side of the station, while the pile body embedded in the lower soil layer is mainly strained on the side facing the soil behind the pile, and the position about the largest bending moments moves down with the continuous downward excavation of the soil. The axial forces about the side pile increase with the excavation of the station soil. This is because the soil at the excavation side of station is unloaded, the soil around the pile body being disturbed, then the side friction resistance provided to the side pile decreases, resulting in the axial forces about side pile increasing.
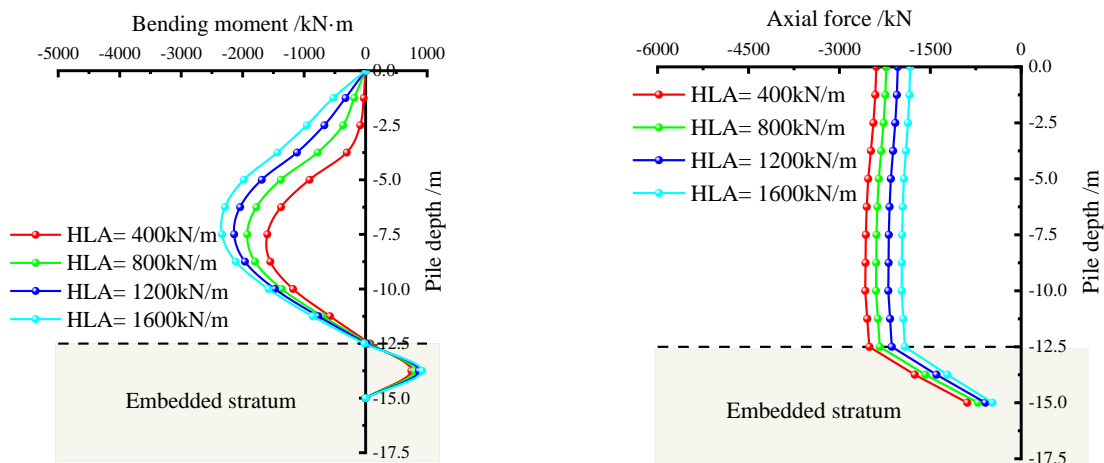
(a) Distribution diagram of bending moments   *(b) Distribution diagram about axial force*
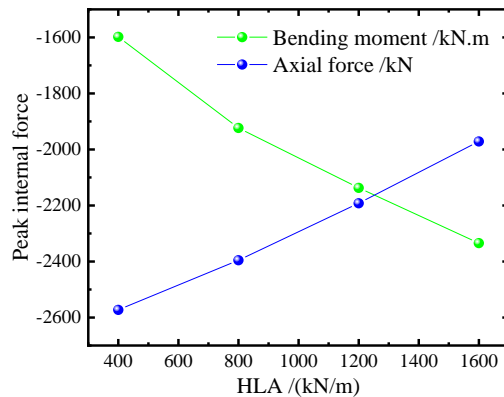
(c) The relationship between the peak internal force and HLA

Fig. 9 - Comparative diagram about the internal force in the final stage of side pile

In Figure 9, with the increase of the HLA, the bending moments of the side pile gradually increases, but the axial force about the pile gradually decreases. Taking the HLA of 400kN/m and 1600kN/m as an example, the bending moments as well as axial forces about the former are -1598.01kN·m and -2573.14kN respectively, and that of the latter are -2334.73kN·m and -1971.78kN respectively, which increase by 46.10% compared with the bending moments. The axial force value decreased by 23.37%, indicating that the impact about the HLA on the bending moments about side pile is greater than that of the axial force.

The influence of VLA on side pile

Deformation analysis of the pile

The evolution rule about lateral displacements of pile structure under different VLA along with the station construction process is displayed in Figure 10, and the final lateral displacements diagram about pile under different VLA after the station construction is shown in Figure 11.

(a) VLA =800kN/m
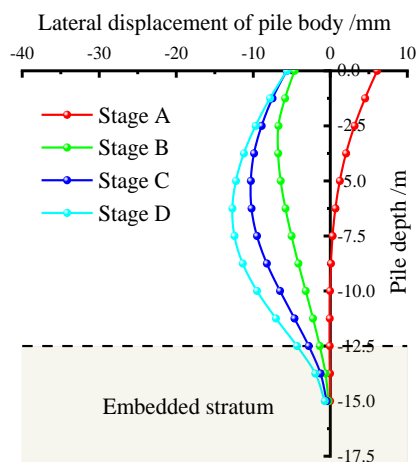
(b) VLA =1200kN/m
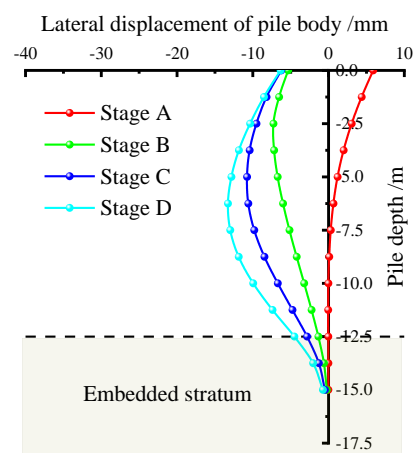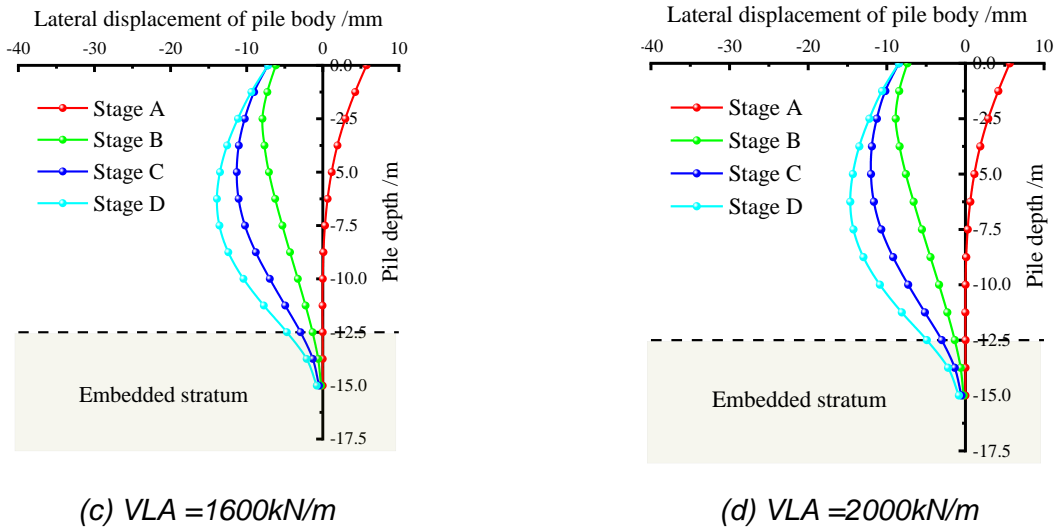
(c) VLA =1600kN/m *(d) VLA =2000kN/m*

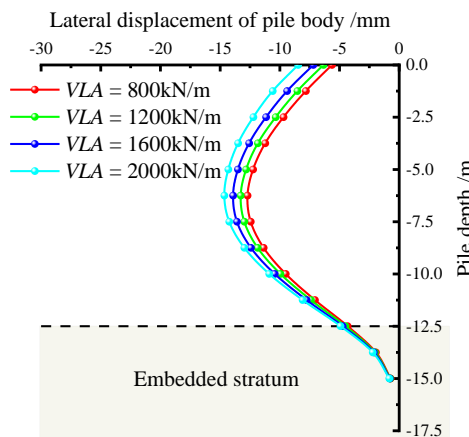*Fig. 10 - Evolution diagram of the lateral displacements about pile under various VLA*

Fig. 11 - Comparison curve about final lateral displacements of pile under different VLA

In Figures. 10~11, the lateral displacements about side pile under different VLA are basically the same, which is mainly manifested as "forward" deformation mode when the buckling arch is completed, and transformed into "bulging" deformation mode after the soil excavation of station. When the VLA is 800kN/m, 1200kN/m, 1600kN/m and 2000kN/m, the final lateral displacement of side piles is 12.70mm, 13.27mm, 13.91mm and 14.64mm in sequence, and the VLA is 2000kN/m compared with 1600kN/m. The lateral displacement increases only by 0.73mm, that is, the final lateral displacements about the side pile gradually adds with the VLA, but the increasing extent is small. This is because the side pile in the station with PBA method is similar to the flexural component, and it is in a "slightly bent state" under the action of the inner soil excavation and the outer soil pressure. The increase of the VLA will increase the eccentric compression of the side pile, and the second-order effect of the VLA will be intensified, resulting in the trend about lateral displacements of pile increasing with the VLA, which is basically consistent with the conclusion of literature [34].

The peak value of lateral displacements about side pile in the final construction stage is

shown in Table 5.

Tab. 5 - Peak value of final displacement of pile body under different VLA /mm

Lateral displacement X /mm	VLA = 800kN/m	VLA = 1200kN/m	VLA = 1600kN/m	VLA = 2000kN/m
Maximum value X_{max}	-0.71	-0.74	-0.78	-0.82
Minimum value X_{min}	-12.70	-13.27	-13.91	-14.64
Relative difference X_d	11.99	12.53	13.13	13.82

In Table 5, the relative difference of lateral displacements about pile gradually adds with the VLA, but the change range is small. When the VLA is 800kN/m, 1200kN/m, 1600kN/m and 2000kN/m, the relative difference of lateral displacement of side pile body is 11.99mm, 12.53mm, 13.13mm and 13.82mm in sequence. It can be found that the difference between the two neighbours is 0.54mm, 0.60mm and 0.69mm, which indicates that the bending degree about pile grows slowly with the VLA.

The variation curves about the displacements of side pile top with the VLA after the completion of station construction is shown in Figure 12.
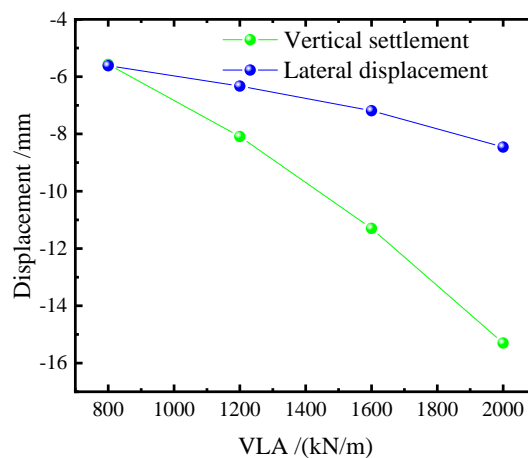

Fig. – 12 Variation curves about the displacements of pile top under different VLA

In Figure 12, under constant HLA, both vertical settlements as well as horizontal displacements about pile top grows with VLA. When the VLA is 800kN, the final vertical settlements as well as horizontal displacements about pile top are -5.57mm and -5.62mm, respectively. When the VLA increases to 2000kN/m, the vertical settlements as well as horizontal displacements about pile top are -15.30mm and -8.46mm, respectively. Compared with the VLA =800kN/m, the increment about vertical settlements as well as horizontal displacements is 9.73mm and 2.84mm, respectively, with an increase of 174.69% and 50.53%, respectively. It reveals that the vertical settlements about side piles is more significantly influenced by the increase of VLA, and the lateral displacements about pile only grows slightly due to the second-order effect of VLA.

Analysis of the variation law about internal forces of pile

The evolution law about internal force of the lower pile structure under different VLA during the construction process is displayed in Figures. 13~14. The distribution of final internal force and peak internal forces diagram about the pile after the completion of the station construction are shown in Figure 15.
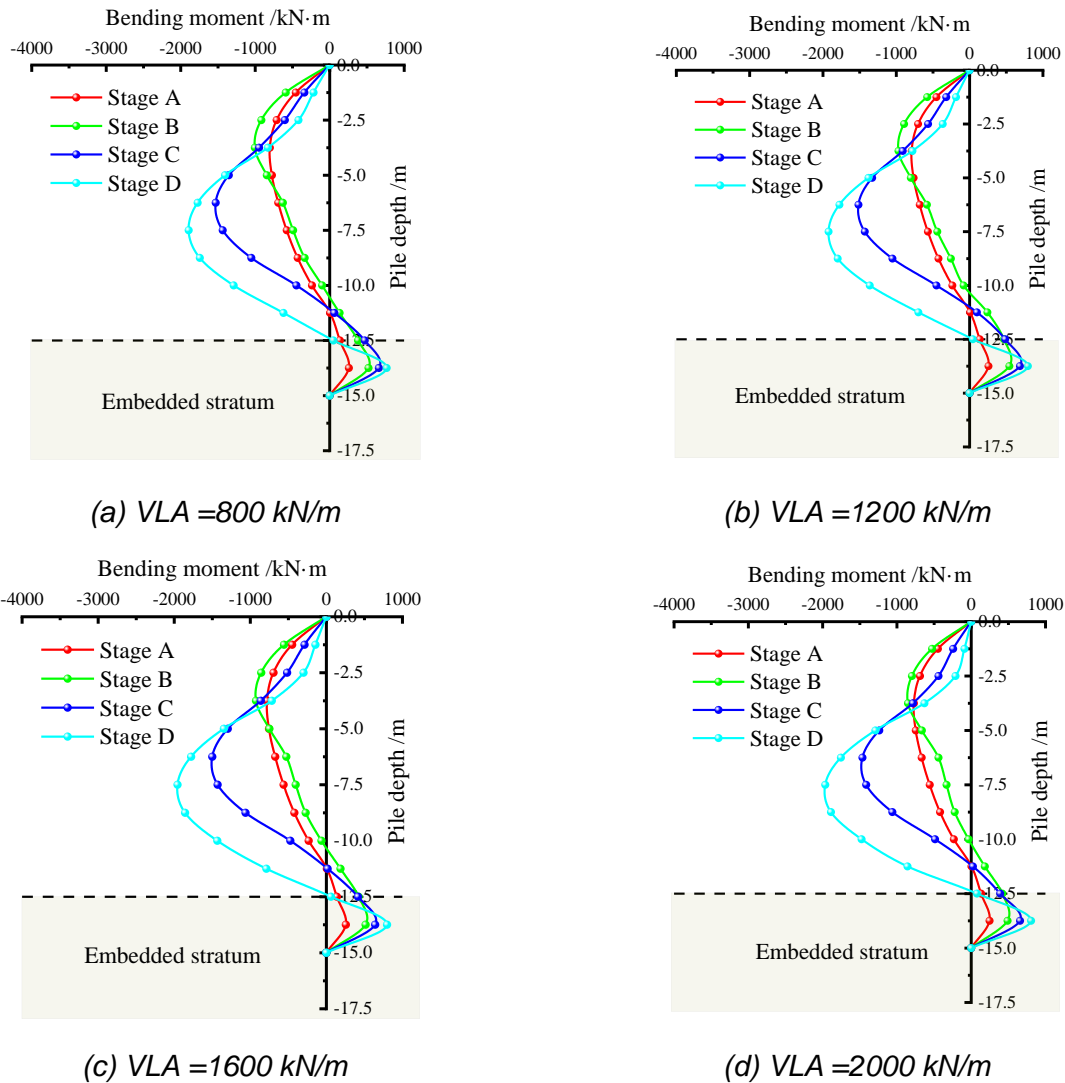

(a) VLA =800 kN/m

(b) VLA =1200 kN/m

(c) VLA =1600 kN/m

(d) VLA =2000 kN/m

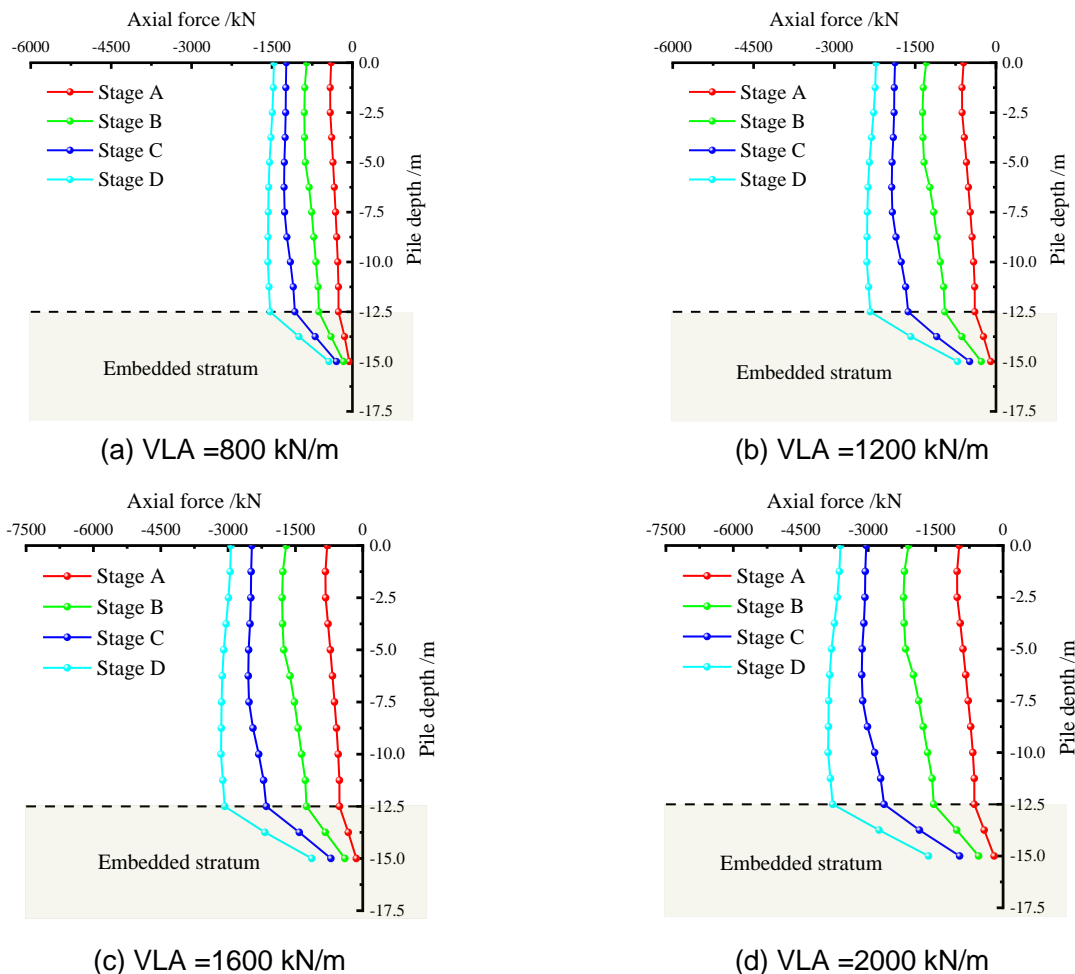*Fig.13 - Evolution of the bending moment of pile under different VLA*

Figure – 14 Evolution diagram of the axial force of side pile under different VLA

In Figs. 13-14, during the construction process of station, the evolution law of internal force of side piles under different VLA is basically the same, and the bending moments about pile are basically presented as a "bow" distribution feature with large in the middle and small at both ends. In addition, the pile above the excavation face is mainly strained on the excavation side of the station, while the pile embedded in the lower soil layer is mainly strained on the side facing the soil behind the pile. The location of the largest bending moments decreases with the continuous downward excavation of the soil. The axial forces about the side pile grows with the excavation of the station soil, this is because the soil at the station excavation side is unloaded and the soil around the pile body is perturbance by the excavation. The side friction resistance provided to the side pile decreases, resulting in the increase of axial forces about the side pile.
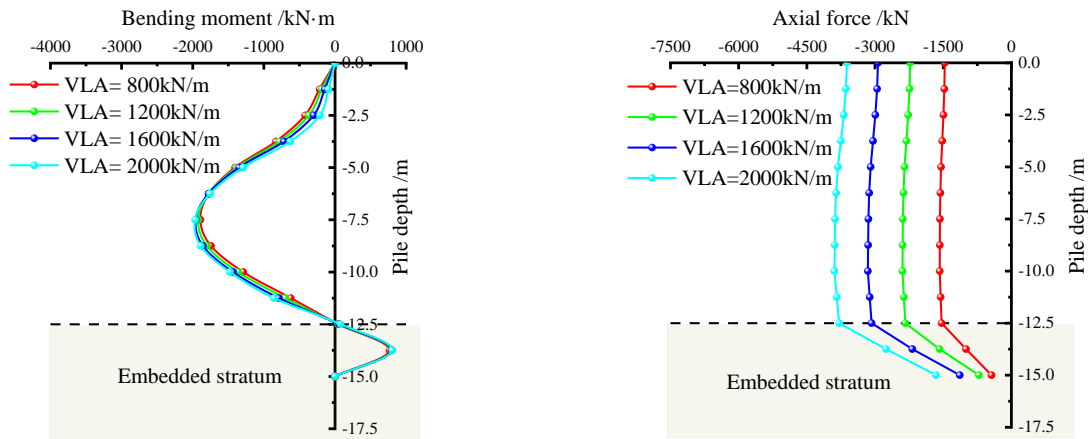
(a) Allocation diagram of the bending moment   *(b) Allocation diagram of the axial force*
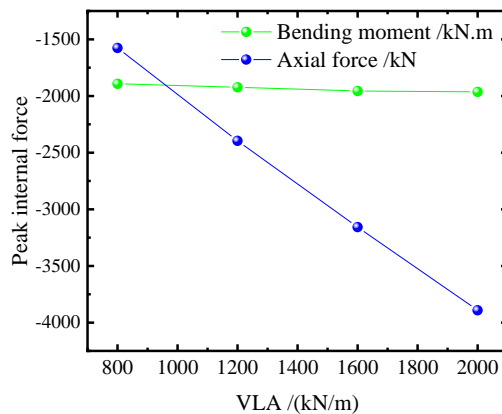
(c) The relationship between peak internal force and VLA

Fig. 15 - Comparison of the final internal force about side pile under various VLA

In Fig. 15, the bending moment and axial force of side pile both increase with VLA. When VLA is 800kN/m, the largest bending moments as well as axial forces about side pile are -1892.21kN·m and -1576.20kN respectively. When VLA increases to 2000kN/m, the largest bending moments as well as axial forces about side piles are -1964.09kN·m and -3891.70kN respectively. Compared with the VLA = 800kN/m, the largest bending moments as well as axial forces increase by 71.88kN·m and 2315.50kN respectively, which increases by 3.80% and 146.90% respectively. It reveals that the increase of VLA greatly affect the axial force of side pile, but little influence on bending moment.

Influence of the SPP on side pile

Deformation analysis about the pile

The evolution rule about lateral displacements of lower pile structure under the action of SPP along with the construction process of station is shown in Figure 16.
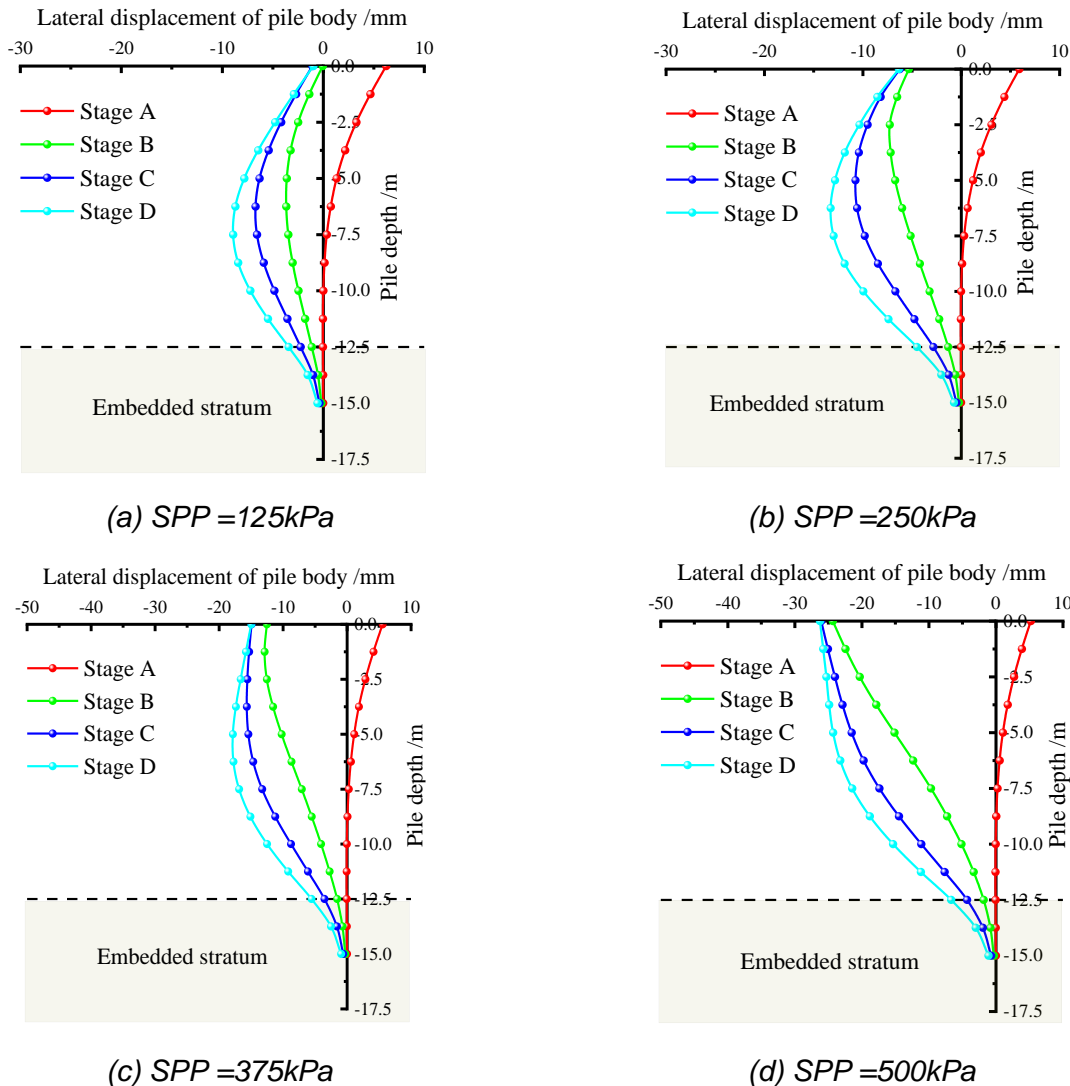
(a) SPP =125kPa

(b) SPP =250kPa

(c) SPP =375kPa

(d) SPP =500kPa

Fig. 16 - Evolution law of lateral displacements about the pile under various SPP

In Figure 16, after the completion of arch, the side pile produces a "forward" type positive displacement to the outside of the station due to the HLA, and with the increase of SPP, the positive displacement shows a gradually decreasing trend. When the SPP is 0.125 MPa, 0.250 MPa, 0.375 MPa, 0.500 MPa, the largest lateral displacements about the pile after the completion of arch all appears at the pile top, and the value is 6.24mm, 5.91mm, 5.57mm, 5.23mm, and the positive displacement gradually decreases. This is because under the action of SPP, the soil behind the pile compresses into the station, which plays a crucial role in restraining the positive displacements about the side pile caused by the HLA. Subsequently, due to the excavation of soil inside the station, the side pile gradually deviates to the station. There is no internal lining system in the side pile when the soil is excavated, and the pile top position is restricted and controlled only by the HLA, VLA and crown beam. With the increase of SPP, the lining effect about the pile top turns into unstable, and the deformation about pile body gradually change from the deformation mode of "bulging" to "backward". When the SPP is large, the lateral soil pressures about the side pile increases, and the HLA and VLA on the side pile top is not enough to resist the SPP, and the instability failure occurs

first at the pile top, leading to large deformation.

The final lateral displacements diagram about pile structure under various SPP after the completion of station construction is shown in Figure 17, and the peak value of lateral displacements about pile under various SPP at the final stage is shown in Table 6.
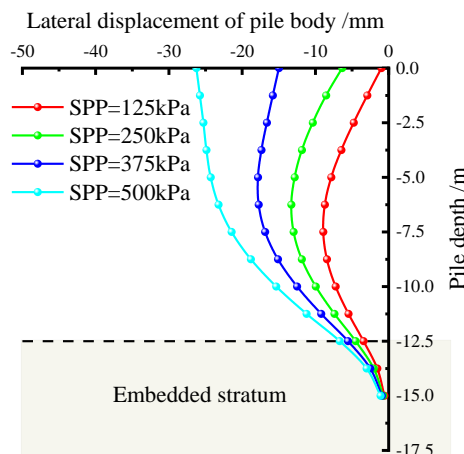

Fig. 17 - Comparison of the final lateral displacements about pile body

Tab. 6 - Peak value of the final displacements of pile under different SPP /mm

Lateral displacement X /mm	SPP =125kPa	SPP =250kPa	SPP =375kPa	SPP =500kPa
Maximum value X_{max}	-0.57	-0.74	-0.92	-1.10
Minimum value X_{min}	-8.92	-13.27	-17.83	-26.24
Relative difference X_d	8.35	12.53	16.91	25.14

In Figure 17, with the increase of SPP, the lateral displacements about the side pile increase, and the displacements about the pile body gradually change from "bulging" type to "backward" type. The position where the maximum lateral displacement occurs shifts from the middle of the pile to the pile top, and side pile begins to show a tendency of instability and failure. Therefore, the corresponding lining system should be set according to the SPP to guarantee the stabilities about side pile during construction.

In Table 6 and Figure 17, with the increase of SPP, the relative difference of lateral displacements about the pile gradually increases, and the change rate about growth gradually accelerates. When the SPP is 125kPa, 250kPa, 375kPa and 500kPa, the relative difference about lateral displacements of side pile is 8.35mm, 12.53mm, 16.91mm and 25.14mm, respectively. It can be found that the difference between the adjacent two is 4.18mm, 4.38mm and 8.23mm, which indicates that the greater the SPP, the greater the relative difference of lateral displacements about the pile, and the more serious the bending degree about the pile, which is more unfavourable to the stability of the side pile. When necessary, lining measures should be taken to strengthen the side pile.

The variation curve about the displacements of pile top with SPP after the completion of station construction is shown in Figure 18.
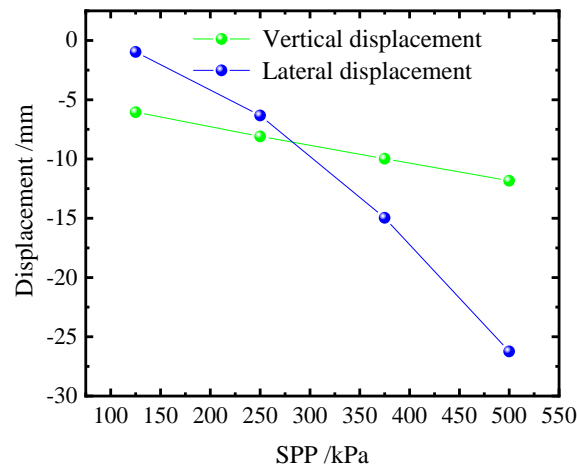

Fig. 18 - The variation curves about the displacement of pile top under different SPP

In Figure 18, with the increase of SPP, the side soil pressure borne by the side pile increases, and the vertical settlement of the pile top increases linearly. This is mainly due to the increasement about the SPP, the soil behind the pile is compressed and compacted, resulting in a certain vertical deformation, and at the same time, the side pile is also subjected to downward settlement deformation. The settlement amount is almost positively correlated with the SPP. Also, the lateral displacement about the pile top grows with the SPP, this is because the lateral lining strength about the pile top is becoming insufficient to resist the side soil pressure behind the pile, and the top of side pile gradually begins to show a trend of instability and failure. When the SPP is 125kPa, 250kPa, 375kPa and 500kPa, the lateral displacements about the side pile top are -0.97mm, -6.33mm, -14.96mm and -26.24mm, respectively, and the difference between the two adjacent piles is 5.36mm, 8.63mm and 11.28mm, respectively. This reveals that the SPP greatly influences the lateral displacements about pile top, and the lateral displacements about pile top grows significantly with the SPP.

Analysis of the variation rule about the internal forces of pile

The evolution curves about internal force of the pile under the action of SPP is shown in Figures 19~20. The final distribution law of internal force about the pile after the completion of the station construction and the comparison diagram of peak internal forces are shown in Figure 21.
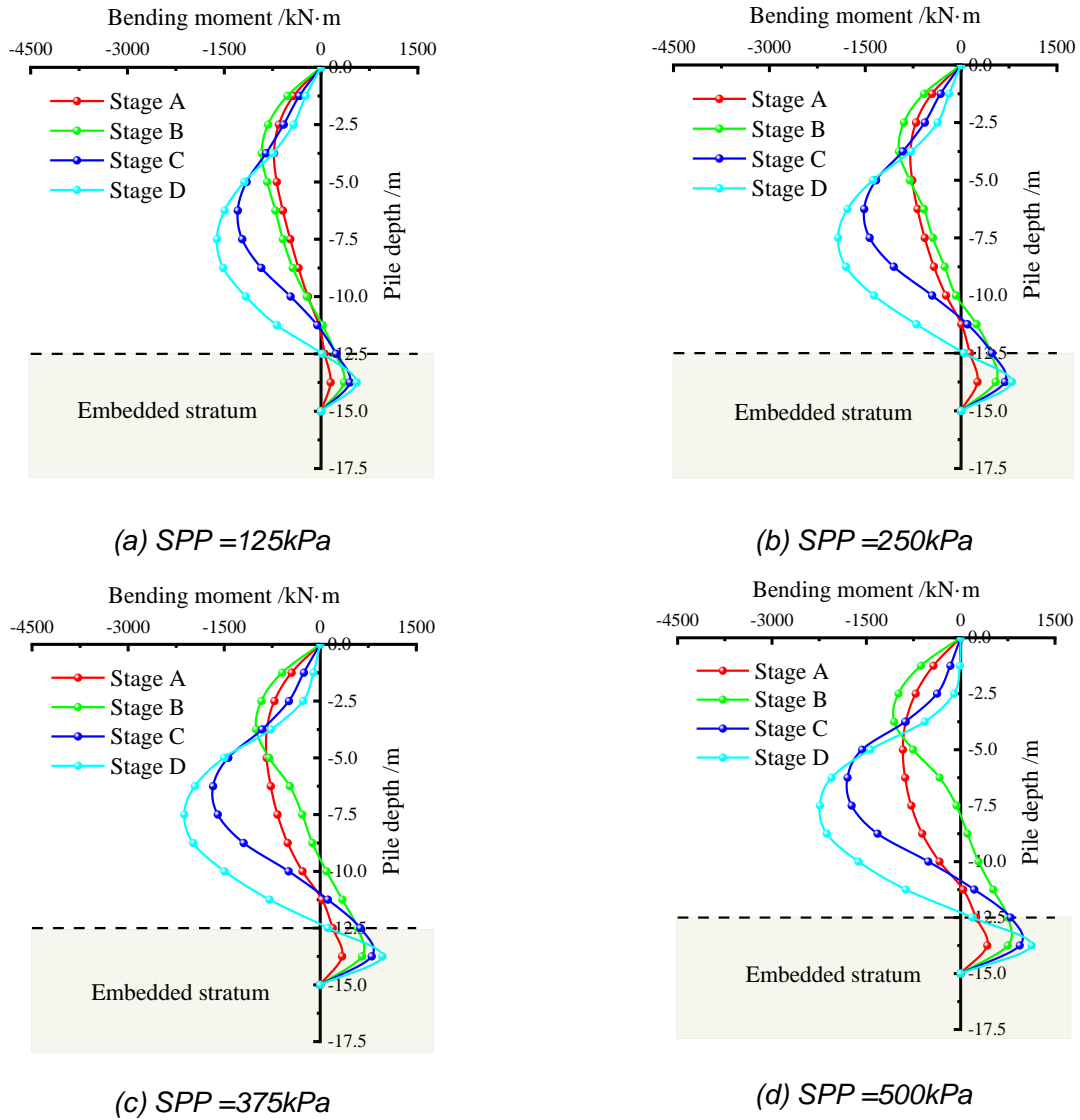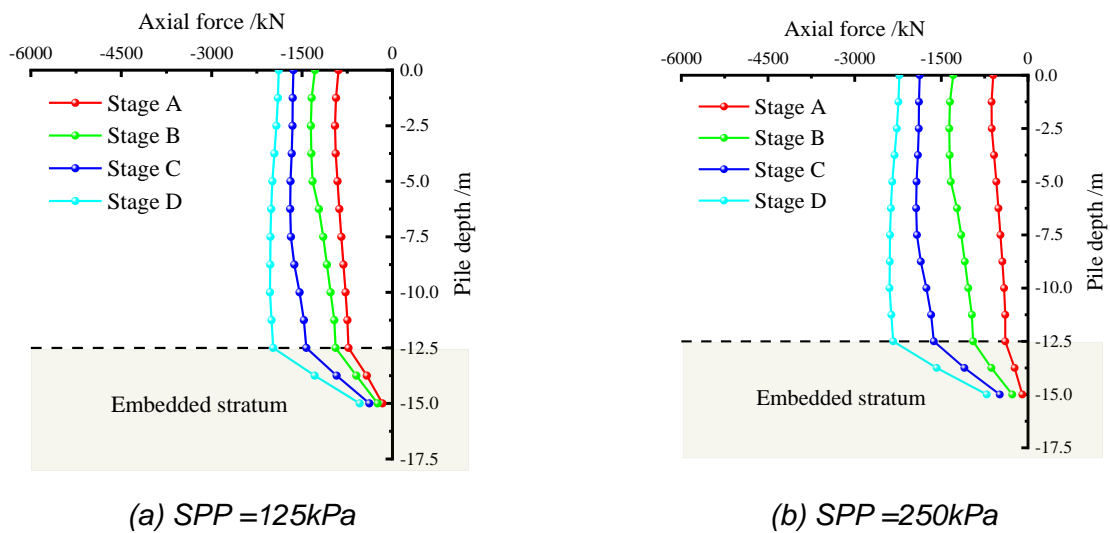
(a) SPP =125kPa

(b) SPP =250kPa

(c) SPP =375kPa

(d) SPP =500kPa

Fig. 19 - Evolution law of the bending moment of side pile under different SPP

(a) SPP =125kPa

(b) SPP =250kPa
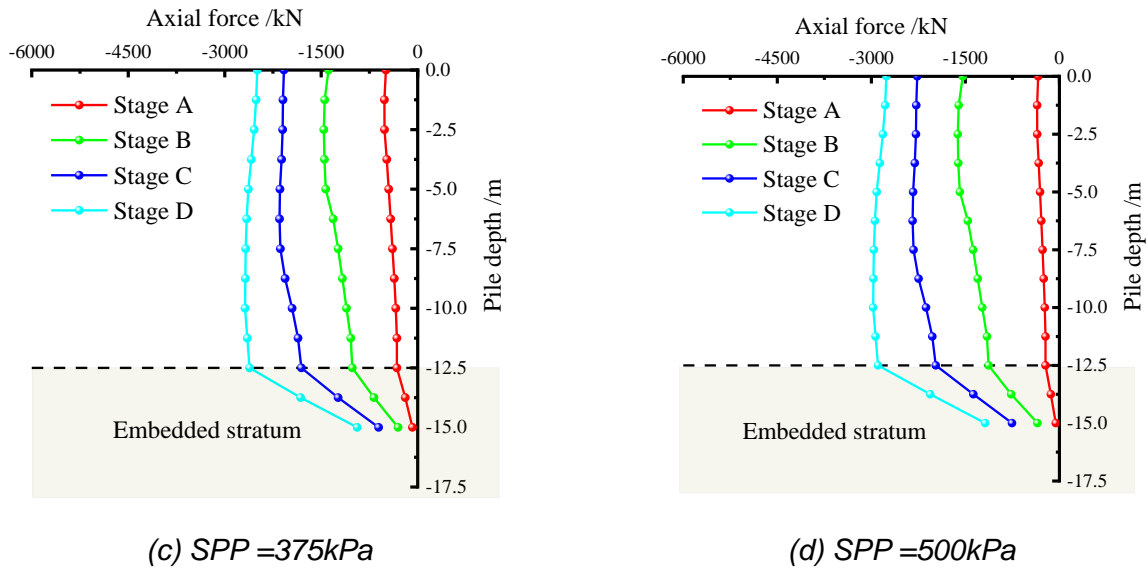
(c) SPP =375kPa

(d) SPP =500kPa

Fig. 20 - Evolution law of the axial forces of pile under different SPP

In Figures 19~20, under the action of SPP, the force morphology of side piles changes with the construction process in a basically consistent way, and the bending moments of piles are presented as "bow" distribution characteristics with large in the middle and small in both ends. The pile body above the excavation surface is mainly strained on the excavation side of the station, and the pile body imbedded in the lower soil layer is mainly strained on the side facing the soil behind the pile. The position about the largest bending moment moves down with the continuous downward excavation of the soil. The axial force of side piles increases gradually with the excavation of station soil. This is due to the soil unloading at the excavation side of the station, the soil around the pile body is perturbate by the excavation, and the side friction resistance provided to the side pile decreases, resulting in the increase of axial forces about the side pile.

(a) Distribution diagram of bending moment

(b) Distribution diagram of the axial force
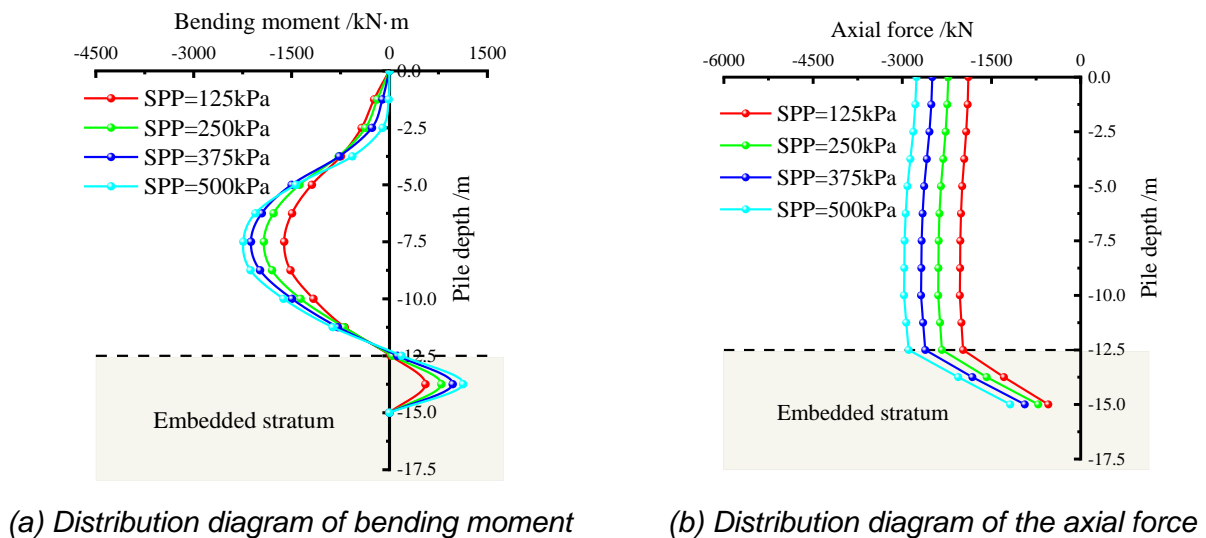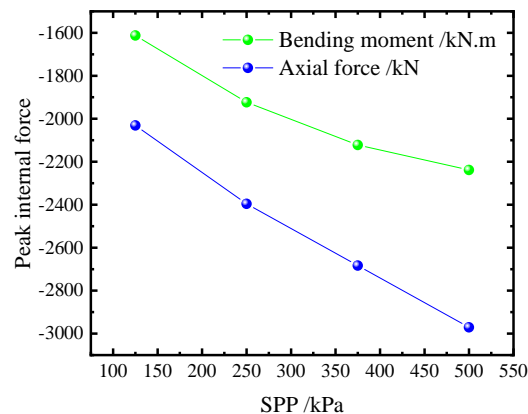
(c) The relationship between the peak internal force and the SPP

Fig. 21 - Final internal force diagram of side pile under different SPP

In Figure 21, the overall bending moments as well as axial forces of the side pile increase with SPP. Taking the SPP =125kPa and 500kPa as an example, the bending moments as well as axial forces about the former are -1612.33kN·m and -2030.96kN respectively. While that of the latter are -2238.49kN·m and -2970.85kN respectively, and the bending moments as well as axial forces increase by 626.16kN·m and 939.89kN respectively. Also, the increase rate of the largest bending moments about the pile decreases with the increase of the SPP. The peak bending moments of side piles under SPP= 125kPa, 250kPa, 375kPa and 500kPa are -1612.33kN·m, -1923.49kN·m, -2121.88kN·m and -2238.49kN·m, respectively. The increments between the two adjacent values are 311.16kN·m, 198.39kN·m and 116.61kN·m, respectively. The peak value gradually increases, but the change rate gradually decreases.

CONCLUSIONS

(1)   HLA has a better control effect on the lateral deformation of the side pile, which effectively ensure the stabilities about the side pile. However, HLA has a relatively optimal value, and too large or too small HLA will lead to greater bending degree of the pile. The allowable value of HLA should be measured according to the actual post-pile load and flexural stiffness of the pile on the site. In this paper, the optimal HLA of the project is 1200kN, and the overall deformation of side piles tends to be more balanced, and the relative difference of lateral deformation is only 10.77mm.

(2)   Compared with the lateral deformation of pile, the VLA significantly affects the vertical settlement of side pile. When the VLA increases from 800kN to 2000kN, the vertical settlement of side piles increases by 9.73mm, while the lateral displacement only increases by 2.84mm, with an increase of 174.69% and 50.53%, respectively. The VLA has a more significant influence on the vertical settlement about side piles, and the lateral displacements about pile body only increases slightly due to the second-order effect of VLA.

(3)   The SPP greatly influences the stability of the side pile, the lateral pressures about soil behind the pile increase with the SPP, and the deformation of pile will change from the deformation

mode of "bulging" to "backward". The top of the pile will easily produce large deformation, and the internal forces about the pile increases. For the case of large SPP, it is recommended to take appropriate lining measures to guarantee the stabilities about the side pile.

COMPETING INTERESTS

The authors have no relevant financial or non-financial interests to disclose.

DATA AVAILABILITY

All data, models, and code generated or used during the study appear in the submitted article.

REFERENCES

[1]   Gao, Y.Q., Xiang, Q.M., Su, J.X., et al, 2022. Strata subsidence characteristics of shield tunneling in coastal soft soil area. Stavební Obzor - Civil Engineering Journal, Vol. 31, 625-635. https://doi.org/10.14311/CEJ.2022.04.0047

[2]   Li, Y.F., Li, J.L., Zhao, J.H., et al, 2023. Research on a safety evaluation system for railway-tunnel structures by fuzzy comprehensive evaluation theory. Stavební Obzor - Civil Engineering Journal, Vol. 32, 122-136. https://doi.org/10.14311/CEJ.2023.01.0010

[3]   Zhang, H.J., Liu, G.N., Liu, W.X., et al, 2023. Stability evaluation of rock pillar between twin tunnels using the YAI. Scientific Reports, Vol. 13, 13187. https://doi.org/10.1038/s41598-023-40167-9

[4]   Zhao, J.P., Tan, Z.S., Yu, R.S., et al, 2022. Deformation responses of the foundation pit construction of the urban metro station: a case study in Xiamen. Tunnelling and Underground Space Technology, Vol. 128, 104662. https://doi.org/10.1016/j.tust.2022.104662

[5]   Wang, T., Luo, F.R., Liu, W.N., et al, 2012. Study of surface settlement and flexible joint pipeline deformation induced by metro station construction with PBA method. China Civil Engineering Journal, Vol. 45, 155-161. (In Chinese). https://doi.org/10.15951/j.tmgcxb.2012.02.005

[6]   Liu, Y.S., Huang, Y.Y., 2023. The surface settlement law of precipitation in pile-beam-arch station adjacent to pile foundation. KSCE Journal of Civil Engineering, Vol. 27, 1441-1457. https://doi.org/10.1007/s12205-023-2192-4

[7]   Li, C.J., 2022. Research on adaptability of PBA improved construction method for underground station in loess area. Railway Standard Design, Vol. 66, 97-104. (In Chinese). https://doi.org/10.13238/j.issn.1004-2954.202102190006

[8]   Zeng, Y., Bai, Y., Zou, Y., et al, 2022. Numerical study on stratigraphic and structural deformation patterns considering surface load with pile-beam-arch method construction. Symmetry, Vol. 14, 1892. https://doi.org/10.3390/sym14091892

[9]   Guo, X.Y., Wang, Z.Z., Geng, P., et al, 2021. Ground surface settlement response to subway station construction activities using pile–beam–arch method. Tunnelling and Underground Space Technology, Vol. 108, 103729. https://doi.org/10.1016/j.tust.2020.103729

[10]   Huang, B., Du, Y.H, Zeng, Y., et al, 2022. Study on stress field distribution during the construction of a group of tunnels using the pile–beam–arch method. Buildings, Vol. 12, 300. https://doi.org/10.3390/buildings12030300

[11] Yu, L., Zhang, D.L., Fang, Q., et al, 2019. Surface settlement of subway station construction using pile-beam-arch approach. Tunnelling and Underground Space Technology, Vol. 90, 340-356. https://doi.org/10.1016/j.tust.2019.05.016

[12]   Li, T., Li, Y., Yang, T.Y., et al, 2023. Influence of the large-span pile-beam-arch construction method on the surface deformation of a metro station in the silty clay-pebble composite stratum. Materials, Vol. 16, 2934. https://doi.org/10.3390/ma16072934

[13]   Wei, Y.L., Ma, H.L., 2023. Load-bearing deformation characteristics and application of reversed micro steel-pipe pile composite foundation. Journal of Anhui Jianzhu University, Vol. 31, 14-18. (In Chinese). https://doi.org/10.11921/j.issn.2095-8382.20230203

[14]   Zhang, J.J., Sui, Q.Q., Guo, M., et al., 2023. Analysis and discussion of the load test of manually

digging piles of Qingdao Jiaodong International Airport. Mechanics in Engineering, Vol. 45, 765-776. (In Chinese). https://doi.org/10.6052/1000-0879-22-573

[15]   Guo, Y.C., Lv, C.Y., Hou, S.Q., et al, 2021. Experimental study on the pile-soil synergistic mechanism of composite foundation with rigid long and short piles. Mathematical Problems in Engineering, Vol. 2021, 6657116. https://doi.org/10.1155/2021/6657116

[16]   Fu, Q., Li, L., 2021. Vertical load transfer behavior of composite foundation and its responses to adjacent excavation: centrifuge model test. Geotechnical Testing Journal, Vol. 44, 191-204. https://doi.org/10.1520/GTJ20180237

[17]   Zhang, D.S., Zhang, X.L., Tang H.T., et al., 2023. Effects of soil arching on behavior of composite pile supporting foundation pit. Computational Particle Mechanics, Vol. 10, 645-662. https://doi.org/10.1007/s40571-022-00518-1

[18]   Liu, X.R., Liu, Y.Q., Yang, Z.P., et al, 2017. Numerical analysis on the mechanical performance of supporting structures and ground settlement characteristics in construction process of subway station built by pile-beam-arch method. KSCE Journal of Civil Engineering, Vol. 21, 1690-1705. https://doi.org/10.1007/s12205-016-0004-9

[19]   Jin, G.L., Wang, Y., Gu, K.Y., 2012. Influence of constructing hand-dug piles closing to retaining wall. Journal of Shanghai Jiaotong University, Vol. 46, 84-88. (In Chinese). https://doi.org/10.16183/j.cnki.jsjtu.2012.01.018

[20]   Liang, R.Z., Wei, S., Wang, X.X., et al., 2022. Comparative test and analysis of the deformation in enclosure structure of internally-braced and cantilevered locked steel-pipe pile foundation pits. Modern Tunnelling Technology, Vol. 59, 172-182. (In Chinese). https://doi.org/10.13807/j.cnki.mtt.2022.03.020

[21]   Chen, Z.Q., Guo, G., Guo, W.X., et al, 2017. Stress characteristics and application of micro steel anti-slide piles. Journal of Lanzhou University, Vol. 53, 43-47. (In Chinese). https://doi.org/10.13885/j.issn.0455-2059.2017.01.006

[22]   Hazarika, H., Watanabe, N., Sugahara, H., et al, 2017. Influence of placement and configuration of small diameter steel pipe pile on slope reinforcement. 19th International Conference on Soil Mechanics and Geotechnical Engineering, Seoul, Korea.

[23]   Xiang, B., Zhang, L.M., Zhou, L.R., et al, 2015. Field lateral load tests on slope-stabilization grouted pipe pile groups. Journal of Geotechnical and Geoenvironmental Engineering, Vol. 141, 04014124. https://doi.org/10.1061/(ASCE)GT.1943-5606.0001220

[24]   Kaczmarek, Ł., Dobak, P., Szczepański, T., et al, 2021. Triaxial creep tests of glacitectonically disturbed stiff clay–structural, strength, and slope stability aspects. Open Geosciences, Vol. 13, 1118-1138. https://doi.org/10.1515/geo-2020-0291

[25]   He, T.F., 2021. Analysis on deformation of foundation pit retaining structure under the condition of CFG pile composite foundation. Subgrade Engineering, Vol. 218, 186-191. (In Chinese). https://doi.org/10.13379/j.issn.1003-8825.20210 3046

[26]   An, G.F., Zhang, H.B., Liu, T.J., 2012. Numerical analysis of bearing characteristics of composite subgrade reinforced by chemical churning pile groups. Rock and Soil Mechanics, Vol. 33, 906-912. (In Chinese). https://doi.org/10.16285/j.rsm.2012.03.049

[27]   Wang, Z., 2018. Research on reinforcement method of loess foundation under existing building. Xi'an University of Architecture and Technology, Master's thesis, Xi'an. (In Chinese).

[28]   Liu, S., Guo, P.P., Li, X., et al, 2023. Settlement behavior of composite foundation with deep mixed piles supporting highway subgrades in water-rich flood plains. Water, Vol. 15, 2048. https://doi.org/10.3390/w15112048

[29]   Benmebarek, M.A., Benmebarek, S., Rad, M.M., et al, 2022. Pile optimization in slope stabilization by 2D and 3D numerical analyses. International Journal of Geotechnical Engineering, Vol. 16, 211-224. https://doi.org/10.1080/19386362.2021.1972628

[30]   Chen, L.J., Jiang, C., Pang, L., et al, 2021. Lateral soil resistance of rigid pile in cohesionless soil on slope. Computers and Geotechnics, Vol. 135, 104163. https://doi.org/10.1016/j.compgeo.2021.104163

[31]   Chen, Y.M., Xu, D.P., 2013. FLAC/FLAC3D foundation and engineering application. China Water and Power Press, Beijing. (in Chinese).

[32]   Huang, F., Li, Z.L., Zhu, L., et al, 2016. The study of ultimate support pressure of shield tunnel face subjected to user - defined constitutive model. Journal of Railway Science and Engineering, Vol. 13, 891-897. (in Chinese). https://doi.org/10.19713/j.cnki.43-1423/u.2016.05.015.

[33]   Jia, F., Du, Y.Q., Yang, W.B., et al, 2023. Research on deformation laws of deeply buried tunnels with small clearance in soft rock by different tunnelling methods. Industrial Construction, Vol. 53, 21-28. (in Chinese).

https://doi.org/10.13204/j.gyjzG22091803.

[34]   Li, T., Gao, Y., Shao, W., et al, 2019. Study on the influence of inclined load on the deformation law of side piles using PBA Method. Chinese Journal of Underground Space and Engineering, Vol. 15, 666-672. (in Chinese).